JOURNAL OF GEOPHYSICAL RESEARCH, VOL. 106, NO. D2, PAGES 1639–1653, JANUARY 27, 2001

Ozone changes in the lower stratosphere from the Halogen Occultation Experiment for 1991 through 1999

Ellis E. Remsberg
Atmospheric Sciences Research, NASA Langley Research Center, Hampton, Virginia

Praful P. Bhatt
Science Applications International Corporation, Hampton, Virginia

Lance E. Deaver
Atmospheric Sciences Research, NASA Langley Research Center, Hampton, Virginia

Abstract. The Upper Atmospheric Research Satellite (UARS) Halogen Occultation Experiment (HALOE) Version 19 ozone profile data set was analyzed for both periodic and nonseasonal polynomial changes in lower stratospheric ozone for 1991–1999. The profile data were screened for cloud contamination at the lowest levels and were then integrated within six half-Umkehr (each ~2.5 km thick) layers from 32 to 253 hPa. The column values were then binned and averaged into 10°-wide latitude regions but separated into sunrise and sunset measurements, yielding an effective time series of zonal-averaged ozone that spans 8 years. The results extend to near tropopause levels, 253 hPa in the extratropics and 127 hPa in the tropics. Multiple linear regression techniques were applied to the data of each latitude zone and half-Umkehr layer. We developed models that included annual, semiannual, and interannual periodic terms plus polynomial terms at 50°N, 30°N, equator, 30°S, and 50°S. The amplitudes of the three periodic terms vary with latitude and pressure altitude and do not maintain their same order of importance in all cases, emphasizing the changes and hemispheric asymmetry of the transport mechanisms in the lower stratosphere. We find no clear evidence for long-term change at most latitudes and layers. Steady declines in ozone of 0.5% yr^{-1} were found in the 32–45 hPa layer at 50°S, most likely due to transport of ozone-depleted air from higher latitudes. Our lowest tropical layer (90–127 hPa) shows an ozone decline in the early 1990s but an increase in the last half of the decade. Steady increases of ozone of 3–4% yr^{-1} were found at 50°N from 127 to 253 hPa and at 30°N from 179 to 253 hPa, probably in response to a changing net circulation for the Northern Hemisphere lower stratosphere. However, there is no highly significant trend at 50°N for the column ozone over the deeper layer from 8 to 253 hPa. For Northern Hemisphere middle latitudes it is concluded that the previously reported declines of zonal-average ozone in the lower stratosphere for the 1980s and early 1990s have not continued over the decade of the 1990s.

1. Introduction and Background

This paper contains an analysis of lower stratospheric ozone variations from the Halogen Occultation Experiment (HALOE) data set. One motivation is to develop an alternate method and independent data set for evaluating the changes in profile ozone from the Stratospheric Aerosol and Gas Experiment (SAGE) II, particularly below 20 km and at latitudes where there are few ozonesonde stations. A second goal is to provide information on changes in lower stratospheric ozone that can be used to interpret the seasonal and longer-term variations in column ozone obtained with ozone sensors on successive operational satellites, particularly in the mid-1990s when there was a nearly 2-year gap in the Total Ozone Mapping Spectrometer (TOMS) ozone time series.

Paper number 2000JD900596.
0148-0227/01/2000JD900596$09.00

Multiyear estimates of seasonal and long-term changes in lower stratospheric ozone have been sought from series of ozonesonde measurements and from series of zonal-mean values from SAGE and SAGE II version 5.96 data [*Cunnold et al.*, 2000a]. Sonde/SAGE II profile intercomparisons indicated good agreement above 20 km (or 50 hPa), but SAGE II was larger than sonde ozone below that level [*Stratospheric Processes and Their Role in Climate* (*SPARC*), 1998; *World Meteorological Organization* (*WMO*), 1999]. Upper Atmosphere Research Satellite (UARS) Microwave Limb Sounder (MLS) version 4 and HALOE version 18 ozone data were used to verify and/or adjudicate those differences below 20 km for 1991–1996 [*SPARC*, 1998]. Again, there was general agreement among the three satellite data sets above the 46-hPa level or the 550 K potential temperature surface. SAGE II is larger than HALOE ozone below those levels; the lower-resolution MLS version 4 data were reported to be inaccurate below the 46-hPa level and not to be a good comparison standard. Improved SAGE II version 6 and MLS version 5 data sets have been generated recently, and they are under evaluation by

others. Preliminary findings indicate better agreement between SAGE II and ozonesonde trends down to 15 km at Northern Hemisphere midlatitudes [*WMO*, 1999]. They also stressed that both the seasonal and nonseasonal trends from ozonesonde time series at middle- and high-latitude stations are not always representative of trends in the zonal-mean ozone, especially during winter and spring [*SPARC*, 1998]. Trends in station data across successive winter seasons are more variable among the sites than for the summer seasons. For instance, a long-term phase shift in a semistationary, wintertime zonal wave pattern would appear as a trend in an ozonesonde station time series. Note that the term "nonseasonal" refers to trends for the annual cycles.

Other satellite data sets can be considered, and the multiyear UARS MLS and HALOE measurements are good candidates. The UARS MLS experiment has provided fairly continuous, multiyear, time series of ozone between about ±34° latitude from late 1991 through 1997, and those MLS data are nearly unaffected by volcanic aerosol contamination. At higher latitudes, MLS also obtained daily samples but with persistent periodic gaps, no shorter than every 36 days according to the yaw cycle of UARS. These gaps make it somewhat difficult to differentiate any long-term ozone changes from the much larger seasonal cycle variations in the extratropics, a region of primary interest in our study. On the other hand, the HALOE measurements are obtained between ±55° latitude fairly regularly throughout the year, although not daily. Thus we report on the periodic variations and long-term changes for 1991–1999 in HALOE version 19 lower stratospheric ozone.

Total column ozone is a proxy for what is happening to ozone in the lower stratosphere, and studies of its large-scale variations have been widely reported [e.g., *McPeters et al.*, 1996; *WMO*, 1999]. For instance, *Randel et al.* [1995] described the changes in column ozone and profile ozone after the eruption of Mount Pinatubo. They found significant decreases in column ozone at middle and high latitudes during winter/spring in the Northern Hemisphere for the period 1991–1993. Their analyses of the HALOE data in the lower stratosphere supported that finding. However, it was still unclear whether the midlatitude changes in ozone were due to the modified chemistry and transport in the period after the Pinatubo eruption and/or whether chemical ozone loss in polar winter/spring was influencing midlatitude ozone. With those issues in mind, we report results for selected latitude zones of both hemispheres based on an analysis of the large-scale variations in a longer, 8-year time series of HALOE ozone. By testing for both linear and quadratic trend terms we will show that there has been no persistent long-term ozone decline for the decade of the 1990s equatorward of 55° latitude, except near 40 hPa at 50°S. This result agrees with the finding that most of the decline in column ozone at those latitudes occurred during the 1980s and in the first few years after the eruption of Pinatubo [see *WMO*, 1999, chapter 4].

Section 2 contains a brief discussion of the quality of the HALOE ozone data and the sampling pattern for the orbital profiles. Section 3 describes how we generated the points that go into our time series of HALOE ozone for a latitude region. Our analysis approach relies on multiple linear regression (MLR), as described in section 4. Results of the analysis are given in section 5 by latitude zone, followed by a brief discussion of the findings in section 6.

2. Description of HALOE Ozone Profiles

The HALOE experiment is described by *Russell et al.* [1993], and the quality of its initial archival ozone profiles (version 17) is reported by *Bruehl et al.* [1996]. The improvements for the HALOE version 18 (V18) ozone are described by *SPARC* [1998], and the measurement errors that could possibly affect its long-term trends are of order 0.07% yr^{-1}. We use the current archival ozone data (version 19 or V19), which is essentially unchanged from V18, except that minor sunrise (SR)/sunset (SS) biases in the V18 solar tracking algorithm were corrected. The individual HALOE profile measurements are sensitive to ozone structure in the atmosphere that has a vertical extent greater than 2.3 km and an azimuthal width of 6 km, although the long, limb tangent path represents a nearly 300-km integration in that direction. Thus the so-called filamentary structure in ozone cannot be resolved well with occultation measurements.

The HALOE ozone channel transmittance data exhibit very good precision and accuracy in the lower stratosphere after mid-1992 [*Bruehl et al.*, 1996]. Whereas the SAGE II visible and near-infrared channel wavelengths are affected primarily by aerosol scattering effects, the HALOE aerosol extinction is due mainly to infrared absorption effects that are based on the aqueous sulfuric acid model of *Hervig et al.* [1995]. They showed that the aerosol correction in the HALOE ozone channel is relatively insensitive to changes in the aerosol size distribution with time. There is only a 0.15% yr^{-1} uncertainty in the V19 ozone trend below 25 km due to the corrections for volcanic aerosol interference after 1992 [*SPARC*, 1998]. *Hervig and McHugh* [1999] developed criteria for screening out those HALOE V19 profile segments that are contaminated by ice particles, clouds, and tropospheric water vapor. *Bhatt et al.* [1999] using similar screening criteria showed that there is good agreement in the lower stratosphere for near-coincident pairs of ozonesonde and screened HALOE ozone profiles.

Figure 1 shows the zonal average of the V19 sunset profiles for the orbital sweep periods of February 26 to April 5 (Figure 1a) and August 24 to October 3 (Figure 1b), 1995. These periods are shown because they extend to high latitudes of both hemispheres but for different seasons. In the lower stratosphere the ozone mixing ratio increases from equator to pole on a pressure surface, roughly following the meridional slopes of the isentropic surfaces. This gradient is due to the effect of the net poleward transport of ozone in the middle stratosphere followed by its descent and accumulation at high latitudes [*Perliski et al.*, 1989]. Figure 1b also shows the effect of the chemical ozone depletion in late winter/early spring of the southern polar latitudes. Because chemistry and diabatic transport processes affect the meridional ozone gradients, one must analyze for seasonal cycle variations in ozone within fairly narrow latitude zones. Furthermore, a gradual speedup or slowdown of the net circulation would appear as a long-term change in ozone at a latitude [*Rosenlof*, 1995].

A remaining concern in analyzing for long-term changes in ozone from HALOE is the ability to account for its much larger seasonal and interannual variations, since fairly frequent and representative sampling is required. Figure 2 is a latitude/time plot of the daily orbital tangent track locations for the SS and SR measurements during 1995. Each point is composed of up to 15 SS or 15 SR profiles for defining its daily zonal average, so the effects of large-scale zonal waves are well

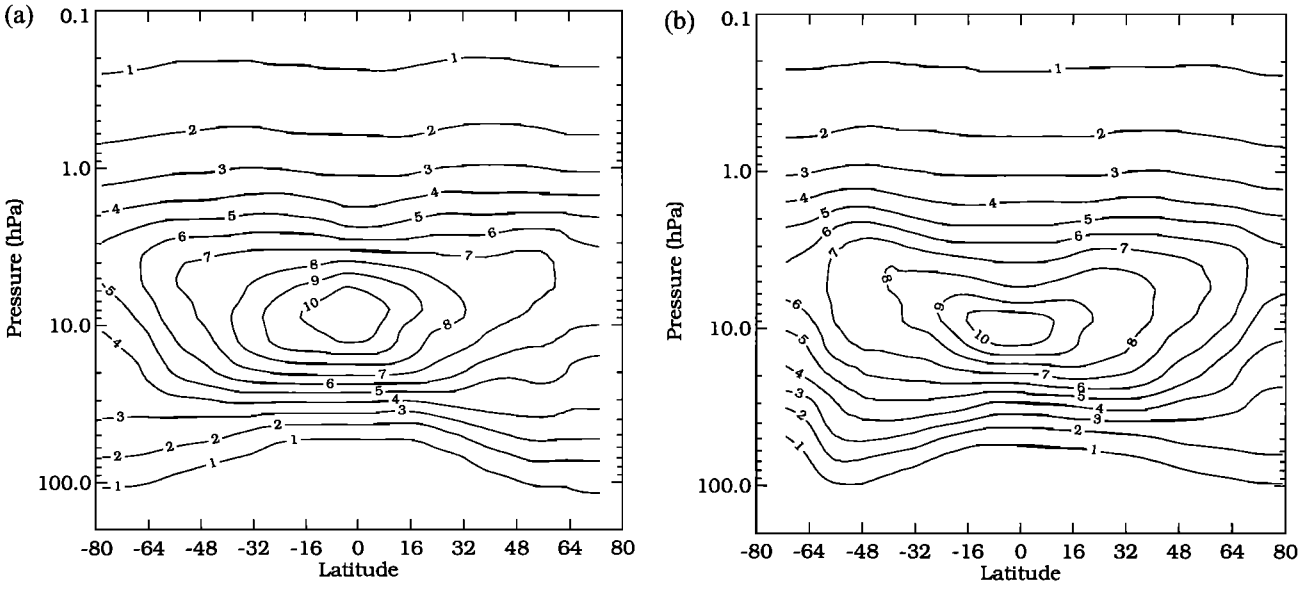

Figure 1. Zonal mean cross section of HALOE SS ozone (in ppmv) for sunset on (a) February 26 to April 5, 1995, and (b) August 25 to October 3, 1995.

represented by this sampling. The HALOE occultations "sweep through" the subtropical and tropical latitudes within a week or so. The middle latitudes are sampled for longer times. Latitudes poleward of ~55° are not sampled for all the seasons. The small dots in Figure 2 trace out the location of the so-called "beta angle" for the measurement, or the angle between the Earth/Sun line and the UARS orbital plane. When the beta angle approaches zero degrees, the spacecraft undergoes a yaw maneuver to reorient its solar panel arrays, and several of the UARS instruments change to Northern Hemisphere rather than Southern Hemisphere viewing or vice versa. At that time the HALOE instrument is normally turned off for several days, and one can see the brief gaps in its tangent tracks in Figure 2. These yaw events occur about every 36 days. Occasionally, the HALOE instrument is turned off to prevent overheating that occurs during near-solar graze angle viewing

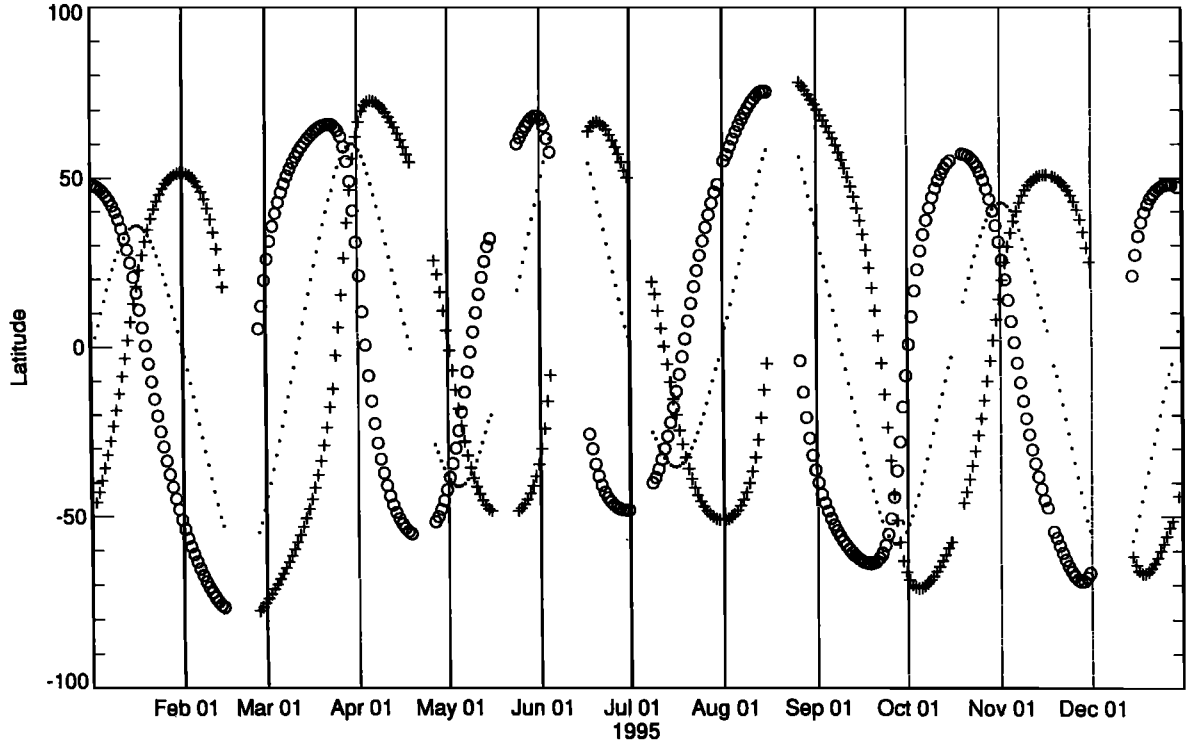

Figure 2. Daily averaged tangent track locations for the HALOE SS (crosses) and SR (circles) orbital segments for 1995. The dotted curve represents the value of the "beta angle" in degrees for the HALOE measurement geometry (see text).

Table 1. Umkehr Layer Pressure Range

Umkehr Layer	Pressure Range, hPa
4U	44.8–31.7
4L	63.3–44.8
3U	89.6–63.3
3L	126.7–89.6
2U	179.1–126.7
2L	253.3–179.1

conditions, and there are data gaps of a week or so during those periods (February, June, August, and December). After mid-1997 the UARS spacecraft was operating without one of its three batteries, and power-sharing arrangements among the UARS instruments had to be implemented. Thus HALOE remained off for several additional days each yaw event during the late 1990s.

3. Ozone Time Series

HALOE V19, level 2, ozone mixing ratio profiles were integrated for constant (~2.5 km thick) pressure layers and then were averaged together within finite latitude bins for the separate SR and the SS orbital sweeps. Analysis of ozone amounts for a pressure layer avoids effects of any long-term temperature changes that would impart a trend in a time series of ozone on an altitude surface. Because the ozone distribution has significant meridional gradients throughout the stratosphere, we considered time series for discrete latitude zones. Profiles for a given orbital sweep were averaged within 10°-wide latitude bins centered at 50° and 30° latitude of each hemisphere. By choosing bins of only 10° width we reduced the effects of a sample bias with latitude within a given bin. We also required a minimum of five profiles for each bin-averaged point to ensure more representative zonal values. Figure 2 shows that HALOE obtains fewer observations at low versus middle latitudes. In the tropical lower stratosphere the horizontal ozone gradients are weak, so we considered a 30°-wide bin centered at the equator (15°N to 15°S) to improve the overall sample statistics for each of its time series points. Latitudes poleward of 55° are not sampled well for all seasons, leading to larger and somewhat irregular gaps in a data time series and a probable bias in its derived seasonal cycle. We did not analyze for large-scale variations at those high latitudes.

We used the higher vertical resolution level 2 profiles in order to more easily search for and screen out the HALOE ozone profile segments whose associated vertical aerosol extinction gradients are large and most likely due to clouds or tropospheric water vapor [*Bhatt et al.*, 1999]. That screening reduced the number of good profile data near the tropopause. During 1991 and early 1992 the post-Pinatubo aerosol extinction limited the lower stratospheric signals of the visible solar tracking sensor of HALOE; ozone profile retrievals were often aborted below ~25 km in that early period.

Random effects in a set of HALOE profiles due to pointing uncertainties reach of the order of 3–10% in the lower stratosphere (16–20 km) [*SPARC*, 1998]. Ozone profile structure is also present due to medium-scale transport processes. Both of those random-like variations are reduced for an ozone time series composed of bin-averaged profile points. To further improve the precision of the points in our time series, we also integrated the HALOE ozone mixing ratio profiles into column ozone amounts for half-Umkehr layers of nearly 2.5 km thickness. Each whole Umkehr layer follows the numbering scheme used for the solar backscattered ultraviolet (SBUV) satellite instrument profiles [*McPeters et al.*, 1984]. In other words, Umkehr layer 4 is 32–63 hPa, layer 3 is 63–127 hPa, and layer 2 is 127–253 hPa. Those layers were then separated into upper and lower halves by log pressure, a thickness that is nearly equivalent to the HALOE retrieval vertical resolution. Those pressure-altitude ranges and layer labels are given in Table 1. Further, by reporting the ozone time series results in terms of layer amounts in Dobson units (DU), it is easier to relate the percentage variations in layer ozone to the changes in total column ozone from SBUV or TOMS.

We analyzed for variations in both the upper and lower halves of Umkehr layers 4–2 (or 32–253 hPa) and for bins in each hemisphere centered at 30° and 50° latitude plus the wider equatorial bin, a total of 30 separate time series. The data time series at tropical latitudes are shown in Figure 3 for layers 4U, 4L, 3U, and 3L along with their MLR model fits (see sections 4 and 5). Cloud screening effectively limits the tropical data from layers 2U and 2L. We looked for significant SS/SR differences when there was near coincidence at ±20° and ±50° latitude (see Figure 2), but we found none for V19 ozone in the lower stratosphere. Thus the combined 117 SS or SR points in the time series of Figure 3 are spaced irregularly but occur with an average frequency of 25 days. Point spacings in Figure 3 for 1995 can be traced back to the low-latitude crossings of the orbital segments in Figure 2. Layer 3L (Figure 3d) exhibits a clear annual cycle. For the higher layers, there is a pronounced biennial cycle plus some higher-frequency variations. We are not attempting to characterize periodic fluctuations that occur with a frequency of <6 months because some short-period features can result from sampling biases for a bin of the occultation data and from the data gaps due to yaw events (every 36 days) of the UARS spacecraft. With only 117 points for the total time series we also did not attempt to analyze for significant trend terms for specific seasons. Therefore the long-term changes that we search for and report are nonseasonal.

4. Analysis Model

By their very nature, the orbital time series data from solar occultation experiments are unevenly spaced after they have been averaged and grouped into latitude bins. For example, SR and SS points often occur within a few days of each other at 20° latitude, followed by a much longer interval before the next point. By simply creating monthly average points from these profiles, as many others have done [e.g., *Randel et al.*, 1999], the true seasonal cycles and the autoregressive (AR) characteristics of the original data set are altered. Instead, we have retained the irregular spacings of the orbital data in time. Basis terms for a linear model fit to those data are nonorthogonal, requiring a time series analysis method that accounts for this generality [*Considine et al.*, 1997, 1999]. Thus we use MLR methods [e.g., *Draper and Smith*, 1967] and apply nonparametric statistical tests [*Press et al.*, 1988] to determine the most significant periodic and polynomial terms in the manner of *Considine et al.* [1999]. Specifically, we require that (1) every model component must be highly statistically significant, (2) variability in the data not captured by the model (the data minus model values or residuals) must satisfy requirements of

the tests for statistical significance, and (3) there must be no evidence of structure in the residuals.

The present analysis of ozone differs from that for the HALOE monthly averaged HF of *Considine et al.* [1997] and the near daily averaged HF and HCl of *Considine et al.* [1999], both at 55 km. Those analyses did not include latitude as a variable in the regression model because the meridional gradients of HF and HCl at 55 km were very small. Ozone has gradients in the lower stratosphere, so our model analysis is performed for latitude bins. Serial correlation is present in our ozone time series but not so much as in the near daily time series of *Considine et al.* [1999]. Finally, periodic structure dominates the ozone time series in the lower stratosphere and must be accounted for accurately when analyzing for any longer-term changes.

Equation (1) is the general form of our linear model used to represent the time series data. It includes a constant, a lag 1 (or $n - 1$) autoregressive (AR) term, polynomial, and periodic terms. The AR term accounts for short-lived correlations in the data. We define linear and quadratic terms in $X = (t_n - t_1)/T$, where t is day number and T is the length of the time series. The periodic terms include semiannual (SAO), annual (AO), and quasi-biennial (QBO) oscillation cycles in Z, where $Z = 2\pi t_n/P$, and P is the period of a given cycle. Parameters a, b, c, d, e, and f are the model coefficients determined by MLR. We do not account explicitly for the effects of the aperiodic El Nino/Southern Oscillation (ENSO) events. We also do not regress against an external 11-year solar cycle index; our data period is between two solar maximums. A solar cycle forcing may not be entirely direct either, but it may have an induced dynamical component that is out-of-phase with lower stratosphere ozone [*Gage and Reid*, 1981]:

$$O3_n = a + bO3_{n-1} + cX + dX^2 + e \sin(Z) + f \cos(Z) + \cdots + \text{residuals}. \quad (1)$$

The steps in our analysis are as follows. An initial model for each latitude and pressure layer includes only the AO term. Then we examined the residuals for any autoregressive character plus any additional periodic structure and then tested a new model that included those terms. The significance of each model term was calculated from the partial correlations between each model component and the data, based on Student's t statistical values for their correlation coefficients [*Press et al.*, 1988]. Specifically, we analyzed terms for significance in their partial rank order correlations (PROC) in the manner of *Considine et al.* [1999]. A Fourier analysis for structure in the residuals does not impose any restrictions about the lack of uniformity in the point spacings. Periodic structure can be highly significant even when there are data gaps.

We carried the significance testing further by correcting for any serial correlation between adjacent data points (i.e., the dependent variable). To do this, we rewrote the dependent variable to account for the lack of independence between data points and tested the significance of the difference partial rank order correlation (dPROC) between this corrected variable and the model term. Each model term was also adjusted by the same correction as to not disrupt the underlying correlation between the data and the model term [*Considine et al.*, 1999]. This AR process, if not corrected for, can otherwise interact with and enhance the significance of the long-period or polynomial terms of the linear model [*Tiao et al.*, 1990; *Weatherhead et al.*, 1998]. Although the MLR procedure does not explicitly account for the variable spacings between adjacent points, it does provide the rank order correlation and significance for AR terms. The AR-1 term was highly significant, except when the data noise was large enough to destroy the memory. We generally set a 99% confidence limit for the PROC of the AR term and the PROC and dPROC of the AO term before they were accepted for the model, a <1% chance that those model terms are purely random occurrences. SAO terms were considered next but were retained only if they were significant at the 95% level or higher in both their PROC and

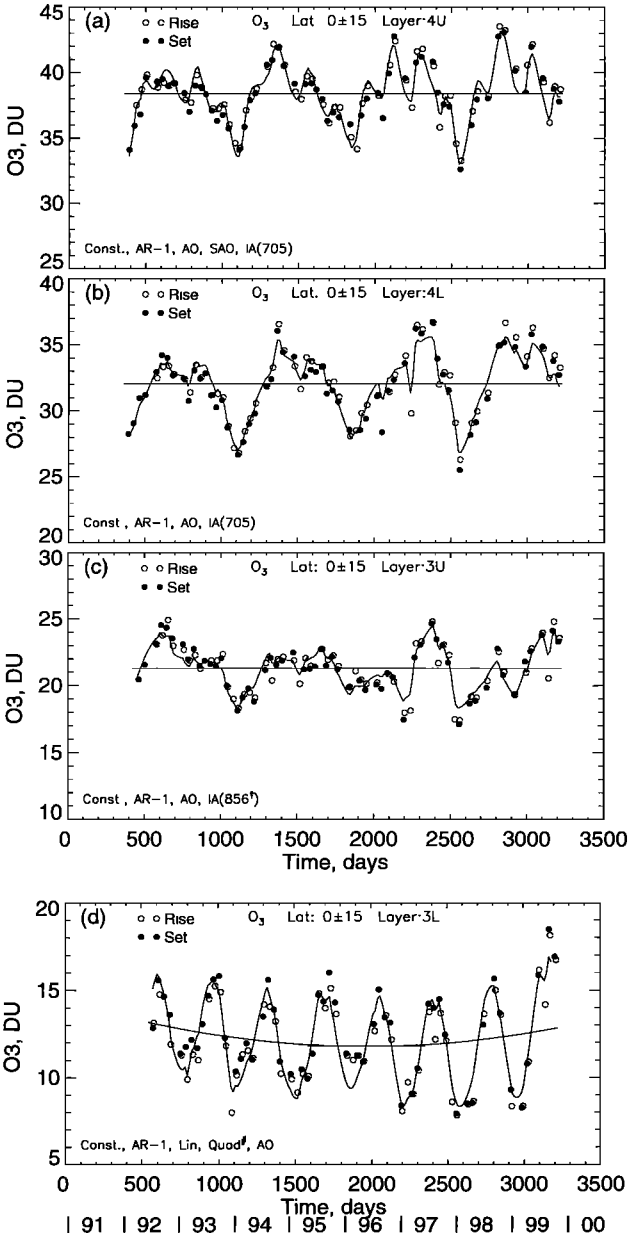

Figure 3. Time series of zonal-average HALOE sunrise (open) and sunset (solid) ozone points in Dobson units (or DU) for half-Umkehr layers and for a latitude bin centered at the equator. The MLR model is shown by the oscillating curve. The superposed curve contains the polynominal and AR-1 terms. Terms are listed at the bottom of each panel, and the IA period is given in days. Layer designations are as in Table 1 and superscript symbols on the terms are defined in Table 3. Abscissa is time in days from January 1, 1991, or by calendar year.

Table 2. Layer 4L for Tropics (0 ± 15) With 117 Data Points, Time Series Mean of 32.04 DU, Start Day 392.13, and Last Day 3212.73[a]

Term	Coefficient	σ	PROC	CI,[b] %	dPROC	CI, %
Constant	11.07	...	...	...	...	...
AR-1	0.66	0.09	0.75	100	−0.22	98
AO	−0.60	0.04	−0.29	100	−0.32	100
IA (705)	0.94	0.14	0.34	100	0.71	100

[a]For lag 1, rank correlation is −0.018, and significance is 15.26; for lag 2, rank correlation is 0.004, and significance is 83.73. The length of data is 2820.59 days, and 74.9% of the data are fitted by this model. The calculated F value is 65.99 and the F distribution table F value is 3.19. PROC, partial rank order correlations; CI, confidence interval; dPROC, difference PROC.
[b]Probability $1 - \alpha$ (see text).

dPROC tests. Next, if interannual (IA) Fourier modes with periods of between 600 and 950 days were found to be significant, we then tested for those terms in the model (see below). Finally, the polynomial (linear and quadratic) terms were added and the testing repeated. Quadratic terms were considered because changes in ozone due to changes in the net circulation following Pinatubo or ENSO events may be reversible.

An example of this analysis procedure is followed for layer 4L of the equatorial bin in Figure 3b. The start day of the time series model is referenced to January 1, 1991 (day 1). The results for this layer are shown in Table 2 and summarized in Table 3 along with the results for the other tropical layers. The model terms include a strong IA term and a weaker AO term (Table 2); the SAO term was not highly significant. The time series mean $\bar{O}_3$ in Table 3 is simply the average of the points and is 32.0 Dobson units (or DU). The complete model (periodic and polynomial terms) that fits the data points is shown as the solid curve. The polynomial terms are shown by the superposed solid line, in this case just the constant term a plus a term defined as $\bar{O}_3$ times the coefficient of the AR-1 term. Note that the sum of those two terms is not exactly equal to $\bar{O}_3$ because the outlier points are not weighted equally in a determination of the term coefficients via PROC methods [*Considine et al.*, 1999]. The period of the IA term was determined by analyzing the residuals for any remaining (besides the AO and SAO periods) low-wavenumber Fourier modes whose rank order correlation was significant at the 95% level. The period of the IA term was calculated from that wavenumber and is 705 days for the model in Figure 3b, somewhat shorter than a QBO period. That period lengthens to 856 days in layer 3U. We note that *Luo et al.* [1997] loosely defined a QBO period to be >520 days, while *Randel et al.* [1998] regressed against the Singapore wind QBO period and *Nedoluha et al.* [1998] regressed against an 825-day cycle. *Tung and Yang* [1994] and *Baldwin and Dunkerton* [1998] found interannual periods of 20 and 30 months at middle latitudes.

At this point we digress briefly to justify our approach to obtaining an appropriate IA term, rather than simply regressing against the QBO cycle in the observed winds. We tested an alternate MLR model IA term based on the empirical cycle of the Singapore winds at 30 and 50 hPa, and we applied it to layers in just the tropical bin to avoid the phase shifts that occur for QBO cycle effects at midlatitudes. The QBO winds have their largest amplitude at 30 hPa. A regression fit to HALOE ozone was carried out at 30, 40, and 50 hPa using that observed wind period. In each case, the QBO-wind term was not significant above the 75% level in the PROCs. On the other hand, our standard Fourier analysis of the residuals yielded an interannual (IA) period of 705–710 days in layer 4. That periodic term was significant at the 99% level for both 4U and 4L. Even though the amplitudes of the residuals were similar when using either the specified QBO or our IA terms, our approach led to an IA term that was highly significant. As one proceeds to the extratropics, the phase of the QBO must be lagged appropriately, adding additional uncertainty for defining its cycle from the observed tropical winds. Our approach to determining an IA cycle accounts for the phase adjustment explicitly for each latitude zone through the coefficients of its fitted sine and cosine terms. The IA periods indicated by the analysis of the Fourier modes were generally preferred for the model. Occasionally, a model with those terms did not satisfy the acceptance criteria, but a slight shift in the IA period did give good results. Those few cases are identified.

Table 2 contains the terms, their coefficients, and standard deviations for the model of tropical layer 4L. Values of the PROC and dPROC plus their confidence intervals (CI) are given in the remaining columns. The CI values are the probabilities $(1 - \alpha)$ in percent that each term is present in the data. We note whether the CI exceeded 99% or at least 95% for each term. Figure 4a shows the autocorrelation coefficients for the residuals for lags 1–59. For example, the lag 1 values are determined from the correlations of the n versus $n - 1$ sequences of points. If the residuals are uncorrelated at a par-

Table 3. Model Terms and Coefficients for HALOE Zonal $\bar{O}_3$ Time Series Latitude of 0 ± 15 (Rise Plus Set)[a]

Layer (CI, %)	$\bar{O}_3$, DU	Constant	AR-1	AO	SAO	IA (Period)	Lin	Quad
4U (99)	38.48	14.65	0.62	0.54	−0.88	0.86 (705)	...	...
4L (99)	32.04	11.07	0.66	−0.60	...	0.94 (705)	...	...
3U (99)	21.33	8.95	0.58	−0.63	...	−0.62 (856[b])	...	...
3L (95)	12.27	9.19	0.43	−1.90	...	...	−8.56	6.97[c]

[a]Center dots indicate that term was absent in the model. Lin, linear; Quad, quadratic.
[b]Period of the IA term is optimized.
[c]Term was present at 95% CI or better but <99% CI.

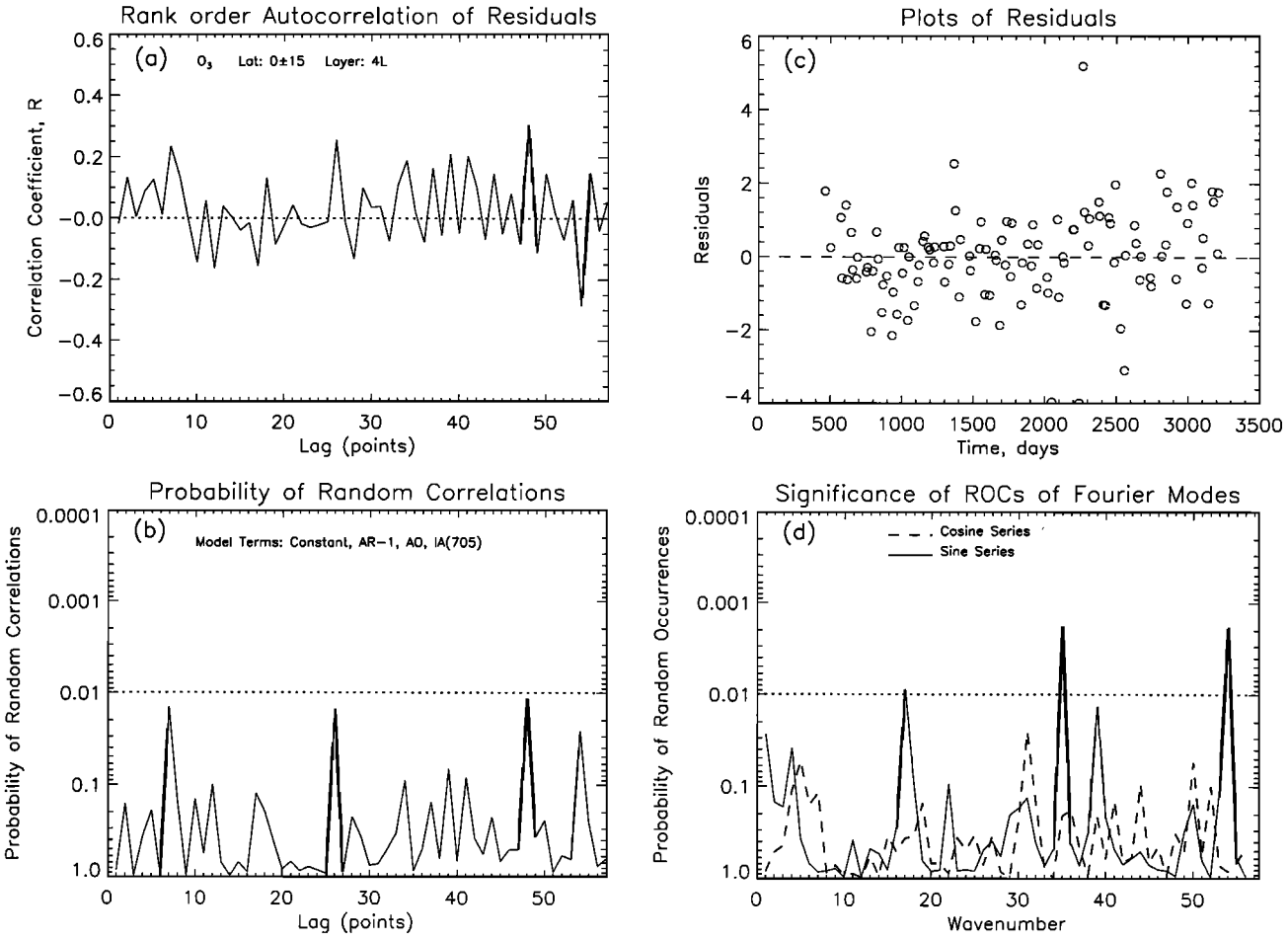

Figure 4. Significance test results for the model of layer 4L in Figure 3. (a) Rank order autocorrelation of the model residuals as a function of the lag in data points—lag 1 occurs at 25 days on average; (b) probability of random correlation, which is everywhere greater than 0.01 or the horizontal dotted line; (c) plot of data minus model values (the residuals in DU); and (d) probability of random occurrences (ROCs) for periodic structure in the ozone residuals. Cosine modes (dashed line) and sine modes (solid line) are shown. The horizontal dotted line indicates that a given mode occurs randomly with a probability of 0.01.

ticular lag number, the correlation coefficient is zero for that AR term. The probability of random correlations is displayed in Figure 4b. The dotted horizontal line is located at 0.01 or the 99% confidence level; significance values that extend below this line indicate that there is a >99% confidence that the correlation coefficient is zero and the residuals are unstructured. Figure 4c is the plot of residuals (in DU) for this model; their average is near zero and their character is essentially unchanged over the length of the time series, as required for model acceptance. The lag 1 and lag 2 correlations that remain in the residuals are listed in the Table 2 footnotes along with their confidence levels. We determined what fraction of the variance (R^2) in the data time series is explained by our final model. The model for layer 4L in Table 2 fits 75% of the data. The related F test value for this model is 66; we use this diagnostic as the final discriminator when more than one model is acceptable. We retested the rank order correlation probabilities of the separate sine and cosine modes in Figure 4d. There is a marginally significant sine peak at 17 wavenumbers (166 days), which is close to an SAO period, but when an SAO term was included in the model, it was not significant at the 95% level. Sine peaks at 35 and 54 wavenumbers correspond to 81- and 52-day periods, and those frequencies remain in the residuals. One or two Fourier modes can occur randomly for our sample size. No other periodic terms are indicated, and no polynomial (or trend) terms are significant at the 95% level.

When an AR-1 term is not included in the model of Table 2, a false linear trend term can be found with a PROC that is significant at the 95% level. However, the residuals at the first few lag points are definitely correlated, and there is periodic structure in the residuals, as shown in Figure 5. Thus that model must be rejected because there is significant structure remaining in the residuals. This example also illustrates the importance of the significance testing that was employed in developing an acceptable model [see also *Weatherhead et al.*, 1998]. In this paper the foregoing analysis steps were followed for each layer and latitude zone. The significance testing was performed separately for each layer to determine which model terms to retain. Continuity of model terms between adjacent layers and latitudes is the most appropriate measure of our success.

Two points are worth mentioning. First, although we included AR-1 terms in our models, there were instances when we still found significant rank order autocorrelation at lag 1 or

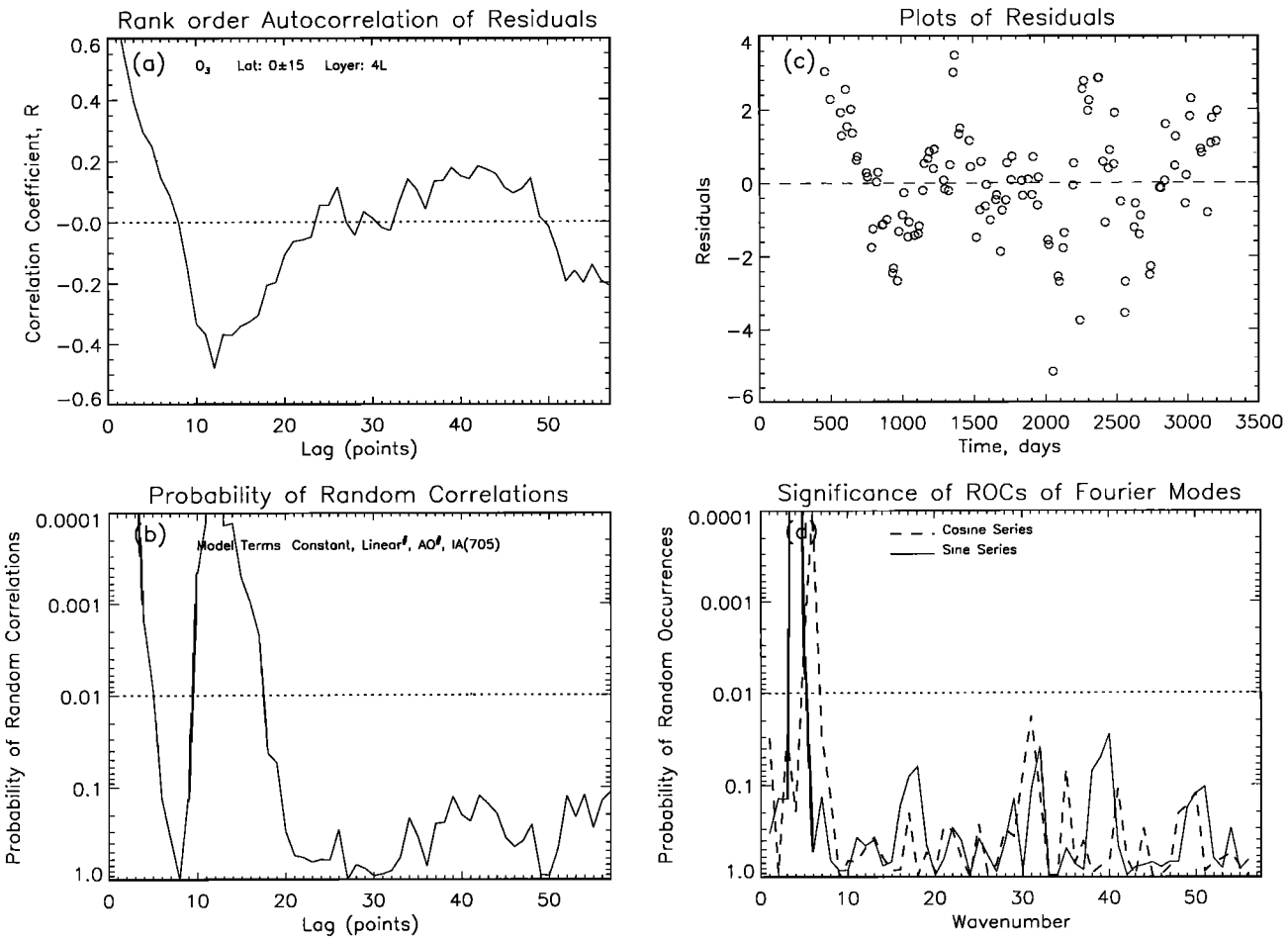

Figure 5. As in Figure 4 but the AR-1 term is replaced by a linear term in the model.

2. This result implies that there are long-period terms or aperiodic terms that are not being fully accounted for. In those cases, further checks for long-period terms and for an aperiodic character in the residuals were not fruitful. It is more likely that we are not always able to accurately model the larger-amplitude AO term with a data time series whose points are spaced a few days to more than a month apart. The analyses of residuals show relatively short period anomalies (as in Figure 4d) that seem to originate from latitude and/or longitude sampling biases within a bin due to missing HALOE profiles. In that instance, if there are also weak, long-period changes in the data for those layers, we may not be fitting them as well. Second, for some layers our final model is not based on the entire length of the data set. At lower altitudes and early in those time series, profiles were either missing or of lower quality because of the effects of the heavy aerosol attenuation of signals in the visible wavelength, solar tracking channel or due to the correction algorithm for aerosol effects. In those instances, we could not find acceptable model terms for the entire time series, so a later start day was sought on the basis of a visual inspection of the point spacings of the time series. Only then could we obtain acceptable MLR fits.

5. Models by Layer and Latitude

5.1. Results for the Tropics

The linear models for tropical latitudes are given in Figure 3 and in Table 3 for the upper and lower parts of layers 4 and 3. Clouds precluded many useful measurements for the full depth of layer 2U and especially 2L. The annual cycle in ozone is very weak in the tropics, perhaps because our tropical bin extends into both hemispheres. Figures 3a and 3b and Table 3 show that the IA term is dominant in layer 4, and Figure 3c for layer 3U indicates a dampening and lengthening of the IA term. In fact, one might conclude that there is not much variation of ozone within this near tropopause layer. Figure 4d indicates the absence of any periodic IA term in layer 3L. This tropopause region is influenced by the seasonal circulation of the troposphere; lowest ozone occurs from December through February, similar to the findings of *Wang et al.* [1998] and most likely due to hemispheric asymmetries of the wave-induced net circulation [*Rosenlof*, 1995].

There is slightly less ozone in layers 4U and 4L in mid-1992 but not thereafter, indicating an early recovery from enhanced tropical ascent of ozone-poor air just after the Pinatubo event and/or from an initial chemical loss of ozone. This result agrees with the findings for Dobson column ozone at Samoa [*Randel et al.*, 1995]. No highly significant, long-term ozone change was found for layer 3U. There is decreasing ozone in layer 3L, most notably in 1997–1998. A recovery occurs during 1998–1999. The start dates for the linear models in Table 3 are increasingly later for layers 3U and 3L due to the attenuation of the solar tracking signal by the volcanic aerosols. However, a polynomial change is present in layer 3L during the remaining years, indicating a long-term change in the wave-induced net circula-

Table 4. Model Terms and Coefficients for HALOE Zonal $\bar{O}_3$ Time Series Latitude of 30°N ± 5° (Rise Plus Set)[a]

Layer (CI, %)	$\bar{O}_3$, DU	Constant	AR-1	AO	SAO	IA (Period)	Lin	Quad
4U (99)	35.67	18.69	0.49	−1.68	···	0.70 (721)	···	···
4L (99)	35.81	14.37	0.60	0.55	···	0.88 (721)	···	···
3U (99)	29.91	9.00	0.69	1.70	···	−0.95 (721)	···	···
3L (99)	25.25	11.70	0.52	2.14	···	−0.82 (740[b])	···	···
2U (99)	5.97	4.29	0.27	1.11	···	···	···	···
2L (99)	4.62	2.39	0.34	0.86	···	···	···	1.34

[a]Center dots indicate the term was absent in the model.
[b]Period of the IA term is optimized.

tion of the lower stratosphere after mid-1996, perhaps following an ENSO event. Because the ozone for layer 3L is only a small fraction of that for the other layers, its effect on total column ozone is small.

5.2. Results at 30°N

Table 4 summarizes the acceptable time series models for each layer at 30°N and the results are shown in Figures 6a–6f. The models are simple and include AO and IA terms but no highly significant polynomial terms except in layer 2L. These findings indicate no long-term change at altitudes within the aerosol layer following the Pinatubo event, although the 1992 minimum in layers 4L and 3U is slightly lower than for succeeding years. We note that the measured ozone signals from SAGE II version 5.96 during this early post-Pinatubo period are not reliable in the lower stratosphere [*Randel et al.*, 1999], although not due to errors in its correction algorithm for aerosol interference [*Steele and Turco*, 1997; *Cunnold et al.*, 2000a]. The HALOE time series for layers 2U and 2L are also not very accurate in 1992.

The screened HALOE results at 30°N yield reliable results after 1992 down to ~13 km and can be used for comparisons with time series of total column ozone. Analogous trends from ozonesondes may not be representative because only one station (Kagoshima) provides a long-term record in this latitude zone. Evidently, heterogeneous chemical destruction and/or large-scale redistributions of ozone following the diabatic heating effects of the aerosol layer must have been confined to the first year or two after the eruption of Pinatubo. According to

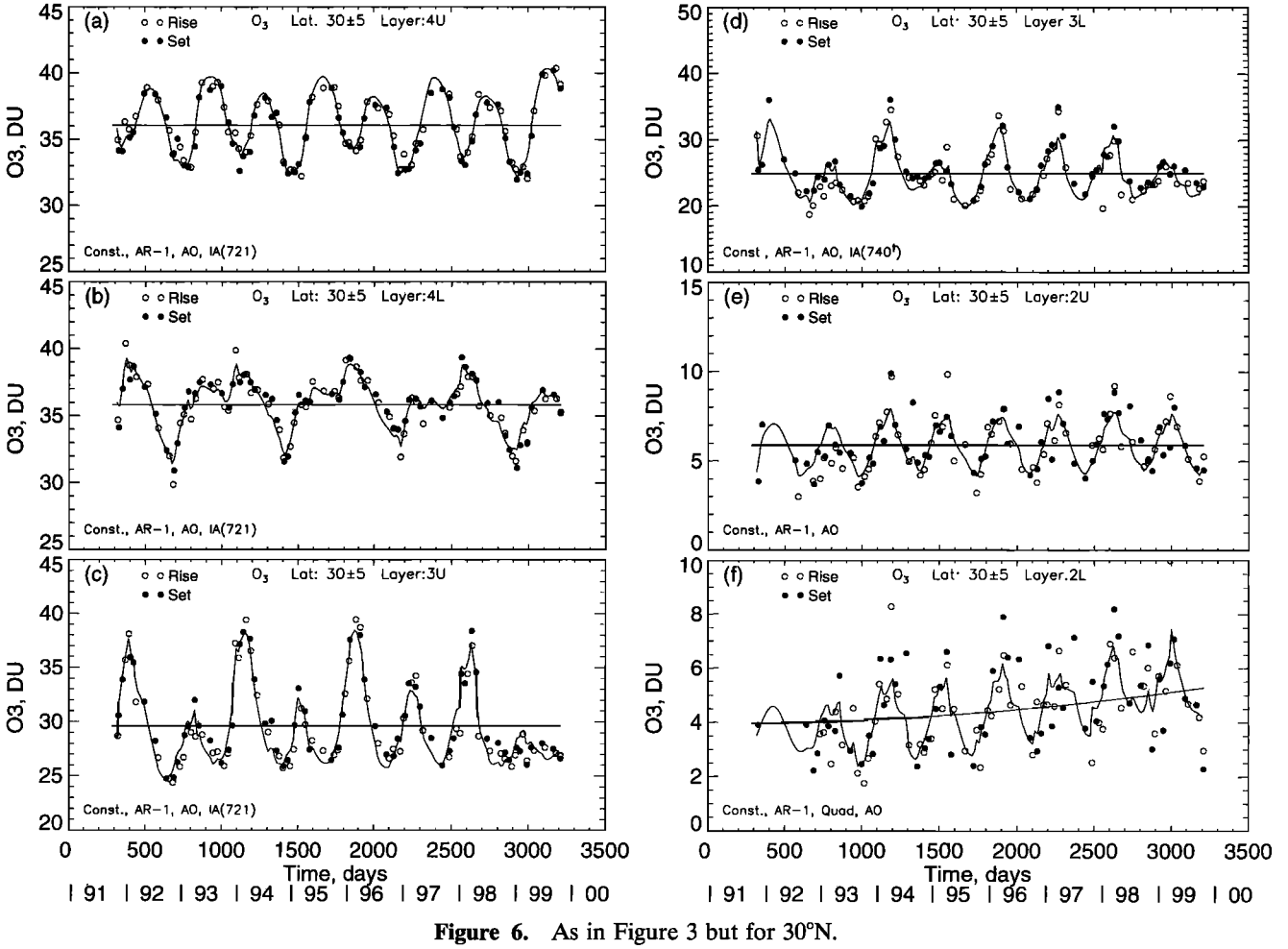

Figure 6. As in Figure 3 but for 30°N.

Table 5. Model Terms and Coefficients for HALOE Zonal $\bar{O}_3$ Time Series Latitude of 30°S ± 5° (Rise Plus Set)[a]

Layer (CI, %)	$\bar{O}_3$, DU	Constant	AR-1	AO	SAO	IA (Period)	Lin	Quad
4U (99)	35.57	14.98	0.58	0.76	···	···	···	···
4L (99)	36.13	19.31	0.46	−2.07	···	0.68 (770[b])	···	···
3U (99)	30.74	15.27	0.48	−4.05	0.89	−0.64 (725)	···	···
3L (99)	26.27	10.02	0.58	−4.66	1.90	···	···	···
2U (95)	5.92	5.52	···	−2.40	−0.53[c]	···	···	···
2L (99)	4.24	4.11	···	−1.34	···	···	···	···

[a]Center dots indicate that term was absent in the model.
[b]Period of the IA term is optimized.
[c]Term was present at 95% CI or better but <99% CI.

the meridional ozone gradients in Figure 1 the steady increase of ozone in layer 2L (3.6% yr^{-1}) indicates an accumulation of ozone poleward of 30°N followed by net descent near the tropopause at middle latitudes during spring [see also *Wang et al.*, 1998; *Fusco and Salby*, 1999]. However, the data time series itself appears to have leveled off after 1998; several more years of data will be required to be sure. The finer-scale structure in the curve for layer 2L is not geophysical but arises from the effect of the large AR-1 coefficient on noisy data (Figure 6f and Table 4).

Both the IA (24 month) and AO cycles are important in the lower stratosphere at 30°N but to varying degrees across the layers. Although the negative anomaly in total column ozone associated with the QBO westerly phase [*WMO*, 1999, Figure 4.7] is present in layer 4L, a positive ozone anomaly dominates in layers 3U and 3L. This changeover for the lower layers occurs just where the springtime meridional gradients in ozone and its transport are pronounced. In this regard, this HALOE analysis provides new details about the role of the QBO in the subtropical lower stratospheric ozone distribution. Clearly, total column ozone cannot be an unambiguous tracer of lower stratospheric transport and stratosphere/troposphere exchange at 30°N. There is a lack of periodic structure in layers 3U and 3L in 1999, yet the linear model follows it well. Although there is destructive interference between the AO and IA oscillations at that

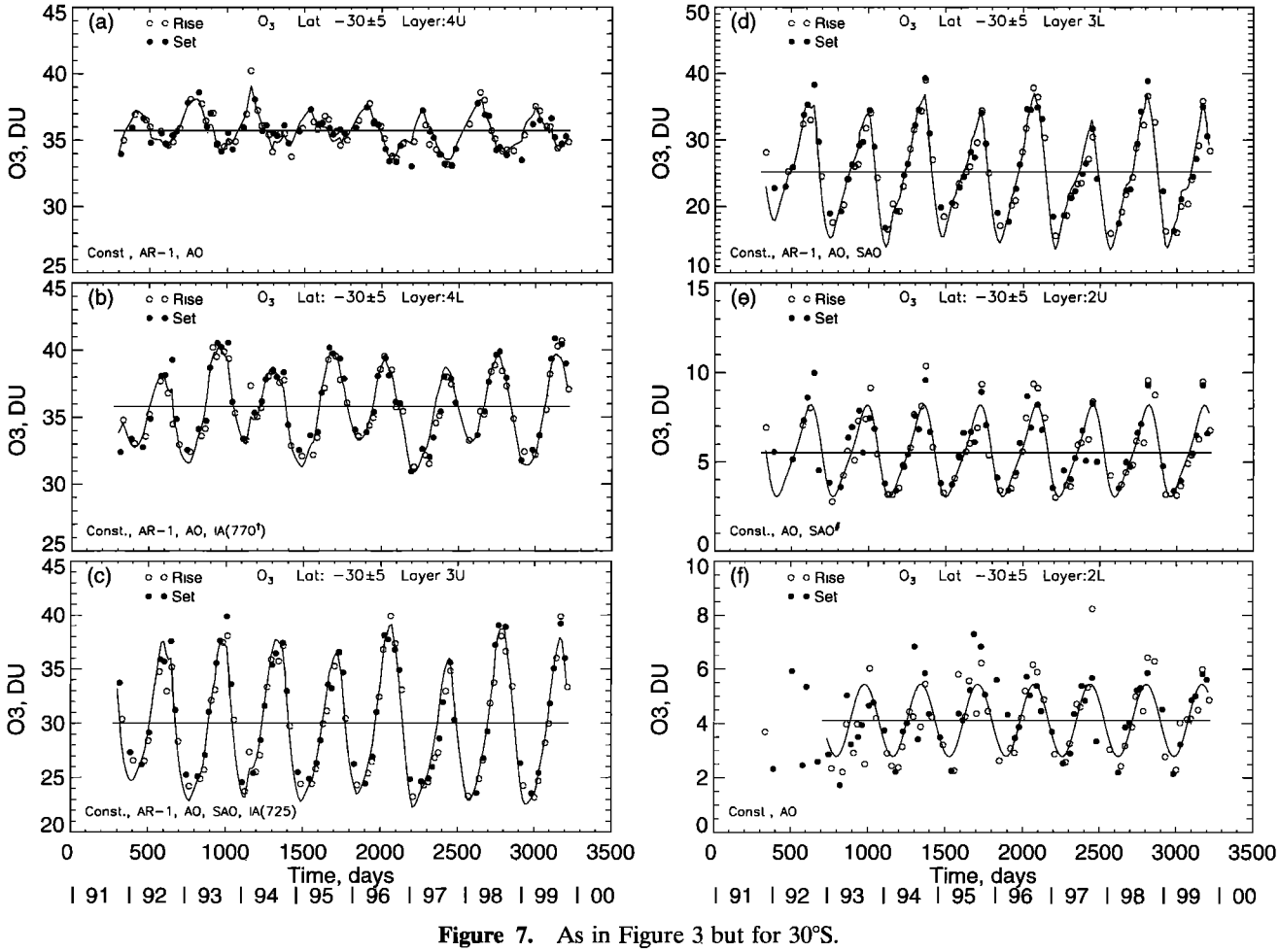

Figure 7. As in Figure 3 but for 30°S.

Table 6. Model Terms and Coefficients for HALOE Zonal $\bar{O}_3$ Time Series Latitude of 50°N ± 5° (Rise Plus Set)[a]

Layer (CI, %)	$\bar{O}_3$, DU	Constant	AR-1	AO	SAO	IA (Period)	Lin	Quad
4U (95)	31.86	25.17	0.25	−0.48[b]	0.96	···	−4.43	3.35[b]
4L (99)	36.71	27.44	0.24	2.73	0.75	0.53 (830[c])	···	···
3U (95)	37.78	31.39	0.14[d]	6.28	0.51[b]	1.53 (765[c])	···	···
3L (99)	49.11	38.30	0.19	10.95	2.08	−1.94 (725)	···	···
2U (95)	23.27	16.36	0.23[d]	5.26	···	−1.21 (770[c])[b]	···	5.28
2L (99)	16.97	7.07	0.36[d]	6.62	···	···	4.62	···

[a]Center dots indicate that term was absent in the model.
[b]Term was present at 95% CI or better but <99% CI.
[c]Period of the IA term is optimized.
[d]Lag 1 autocorrelation is 95% or higher even with AR-1 term included in the model.

time, it is the AR-1 term that provides for the excellent fit to those points. The IA term is not significant in layers 2U and 2L, an indication that QBO effects do not extend below tropical tropopause altitudes.

5.3. Results at 30°S

Table 5 and Figures 7a–7f contain the model terms for the lower stratospheric layers at 30°S. Generally, we find seasonal symmetry with the data time series signatures at 30°N and their linear models (see Table 4) but with some important differences. A weak SAO term is present in layers 3U, 3L, and 2U at 30°S but not 30°N, and the IA term is absent in layer 4U at 30°S. By comparing the model fits in Figure 7 with those in Figure 6, one can see that the effects of the IA term are clearly different for layers 4L, 3U, and 3L. The annual cycle is dominant at 30°S, and it is not interfered with in 1998–1999 as it is at 30°N. Significant IA terms are absent in layer 2U and 2L at 30°S and 30°N, but ozone remains steady in layer 2L at 30°S. The disparities between the models for the two hemispheres emphasize the effects of the larger role of the QBO and planetary wave activity on Northern Hemisphere ozone, especially in winter/spring. There is an interesting feature that shows up in Figure 7e for layer 2U. The MLR model curve has minima that fit the points very closely, while the curve maxima appear to fit the points less well. This character is because the minima are occurring in Southern Hemisphere summer when there is little variation in the ozone field. Although the meridional ozone gradients are more variable for the winter/spring maxima, the model still fits through those points very well. In the early part of the time series for 2L the integrated ozone is less accurate and at times incomplete, and the analysis was started from day 746 (late 1992). Even so, the remaining time series appears noisy, and the AR-1 term is not highly significant.

5.4. Results at 50°N

Table 6 and Figures 8a–8f show the model results for 50°N. The time series for layer 4U in Figure 8a has a much different character than that for layer 4L in Figure 8b. The SAO term, though weak, is the most significant periodic term in layer 4U. *Baldwin and Dunkerton* [1998] found that the SAO term was also dominant for potential vorticity at 30 hPa. At this latitude and pressure the meridional gradients of ozone, while nearly flat, seem to be changing sign with a seasonal cycle (see Figure 1). A long-term loss of ozone is indicated (-0.43% yr^{-1}) in layer 4U, and the polynomial fit in Figure 8a indicates that the losses were mainly in the first half of the 1990s. The more frequent, wintertime chemical losses of polar ozone reported by *Mueller et al.* [1997] must have their zonal-averaged effects confined to latitudes higher than 55°N. There is no long-term trend in zonal mean ozone in layers 4L, 3U (Figure 8c), and 3L (Figure 8d); the zonal effects of polar ozone losses do not extend to the 50°N bin below the 45-hPa level. Figure 8e for layer 2U indicates clearly increasing AO maxima after 1994 and a trend of $+3.4\%$ yr^{-1} from 1991 through 1999. Layer 2L (Figure 8f) also shows significant increases since 1992 ($+3.7\%$ yr^{-1}). The AO term for that layer overestimates the seasonal amplitudes in the early 1990s and underestimates it in the late 1990s because the AO term is an average for the 8-year time span of the model fit. The rather poor fit to the high ozone values for late winter/early spring of 1998 and 1999 is partly the effect of the reduced weighting of "outlier" points by the PROC. For those years, there seems to be enhanced wintertime descent [*Pan et al.*, 1997; *Fusco and Salby*, 1999], which is not accounted for by our set of terms.

The model terms were arranged in Tables 3–6 by layer, and there is model consistency between adjacent layers for 50°N. The empirically determined IA term is significant in layers 4L through 2U, although its period is greatest in layer 4L (27 months). Figure 8b shows no trend in layer 4L and agrees qualitatively with the insignificant trend at 50°N and 46 hPa from SAGE II from 1991 to 1996 [*Cunnold et al.*, 2000b, Figure 8]. The amplitudes of the AO terms in our Figure 8 also compare well with those obtained from the climatology of ozonesonde profiles near 50°N [see *Logan*, 1999, Figure 6]. The agreement for these intercomparisons represents an independent assessment of the quality of the HALOE profiles. The HALOE results for layers 3 and 2 provide new estimates of long-term, zonal-mean ozone change at middle latitudes of the lower stratosphere.

5.5. Results at 50°S

Acceptable models (Table 7 and Figure 9) were found for each layer at 50°S, a zonal region where there is only one ozonesonde station (Lauder, New Zealand) monitoring long-term changes. Layer 4U has SAO and AO terms but no highly significant IA term. We find a clear linear decrease of ozone (-0.5% yr^{-1}) in layer 4U (Figure 9a), but none in the other layers. The effect in layer 4U (Figure 9a) is most apparent as a decreasing ozone maximum after each final warming (see Figure 8a). We interpret this result as an upward and equatorward expansion of the polar ozone hole phenomenon into the 32 to 45 hPa layer during the 1990s. Like the HALOE result, the zonal mean SAGE II data show a decreasing trend of nearly 0.4% yr^{-1} at 45°S for the period 1986–1996 [*Cunnold et al.*, 2000a], while *Bodeker et al.* [1998] found station ozone trends that were increasing at this level for Lauder. However, both of those trend results have 2σ values that include zero at 20 km. Perhaps the negative ozone trend is more apparent for

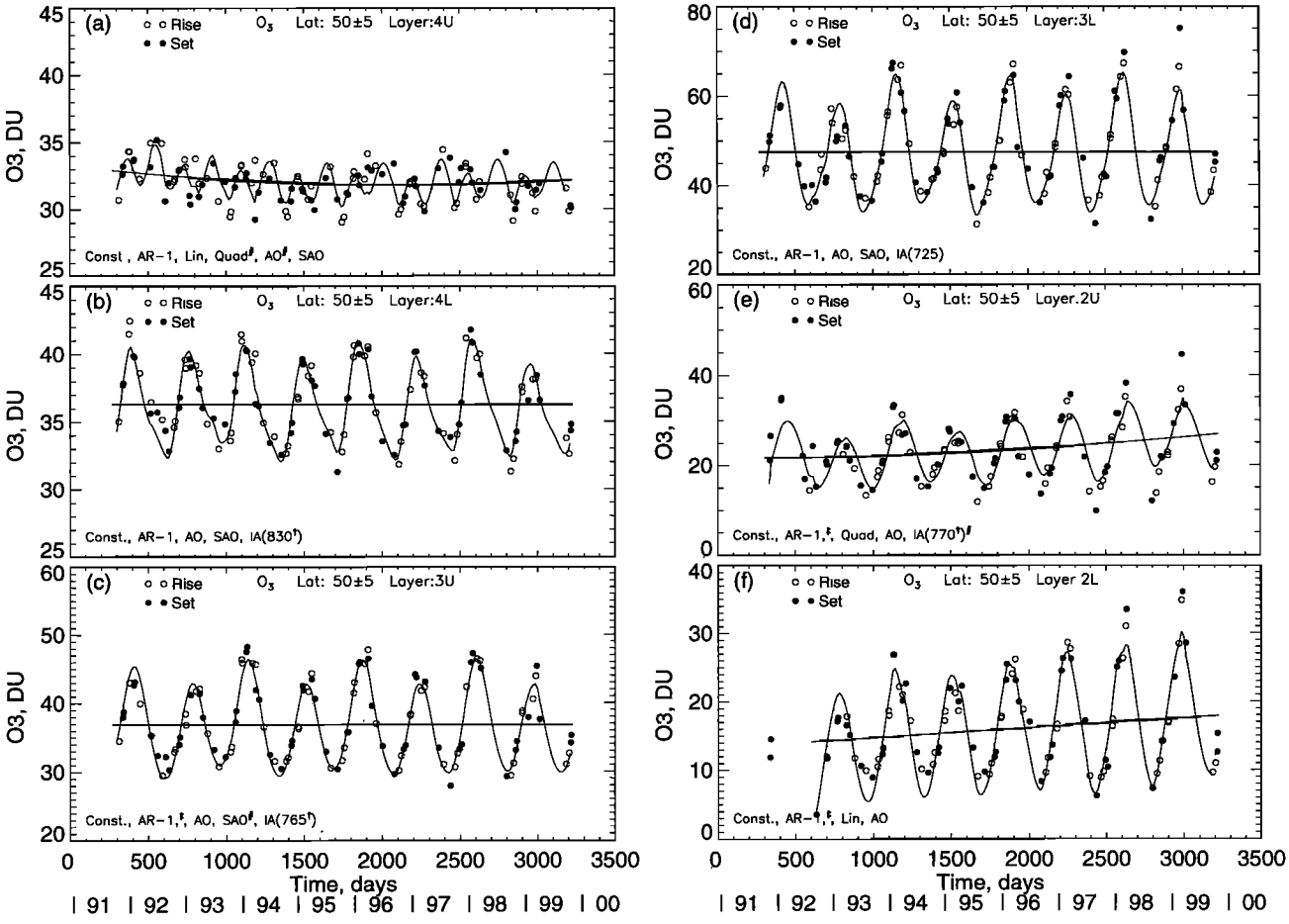

Figure 8. As in Figure 3 but for 50°N.

the more poleward 50°S bin of HALOE or the trend at 50°S is becoming more pronounced in the 1990s. We find no indications of springtime polar ozone losses extending to 50°S in the 45 to 253 hPa region.

Our initial expectation was that seasonal asymmetry between 50°S and 50°N ought to be more apparent than for 30° latitude because of the timings of the final warmings in the two hemispheres and the occurrence of a larger, more persistent ozone hole in southern than northern polar regions. That expectation was not realized. The time-averaged ozone in layers 3U and 3L (Figures 9c and 9d) at 50°S is very similar to that at 50°N, although the AO amplitude is larger at 50°N. Our finding of no trend at 20 km (layer 4L) is at odds with the SAGE version 5.96 result of Figure 2.28 of *SPARC* [1998] that showed a change of −4% per year from 1991 through 1996. Because we were able to detect a −0.5% yr^{-1} trend in the adjacent layer 4U, we would have seen a much larger trend in layer 4L if it had occurred. *Cunnold et al.* [2000b] report no trend at 46 hPa and 50°S from the SAGE version 5.96 data after they deleted its post-Pinatubo measurements up to 1993. Their SAGE trend agrees with the findings from HALOE.

6. Discussion and Conclusions

Total column ozone measurements at northern midlatitudes indicate a loss of ozone for the first year or two after the

Table 7. Model Terms and Coefficients for HALOE Zonal $\bar{O}_3$ Time Series Latitude of 50°S ± 5° (Rise Plus Set)[a]

Layer (CI, %)	$\bar{O}_3$, DU	Constant	AR-1	AO	SAO	IA (Period)	Lin	Quad
4U (99)	31.58	26.09	0.20	−1.11	−0.61	···	−1.17	···
4L (99)	36.08	28.23	0.20[b]	−2.67	···	···	···	···
3U (99)	36.89	30.01	0.17	−4.99	···	−0.70 (721)	···	···
3L (99)	45.89	40.34	0.09	−8.80	−2.03	−2.32 (790[c])	···	···
2U (99)	19.41	15.87	0.12	−5.02	···	−0.86 (710[c])	···	···
2L (95)	13.10	11.07	0.07[b,d]	−4.84	0.91	−0.71 (702[c])	···	···

[a]Center dots indicate that term was absent in the model.
[b]Lag 1 autocorrelation is 95% or higher even with AR-1 term included in the model.
[c]The IA period has been optimized.
[d]Term present at 95% CI or better but less than 99% CI.

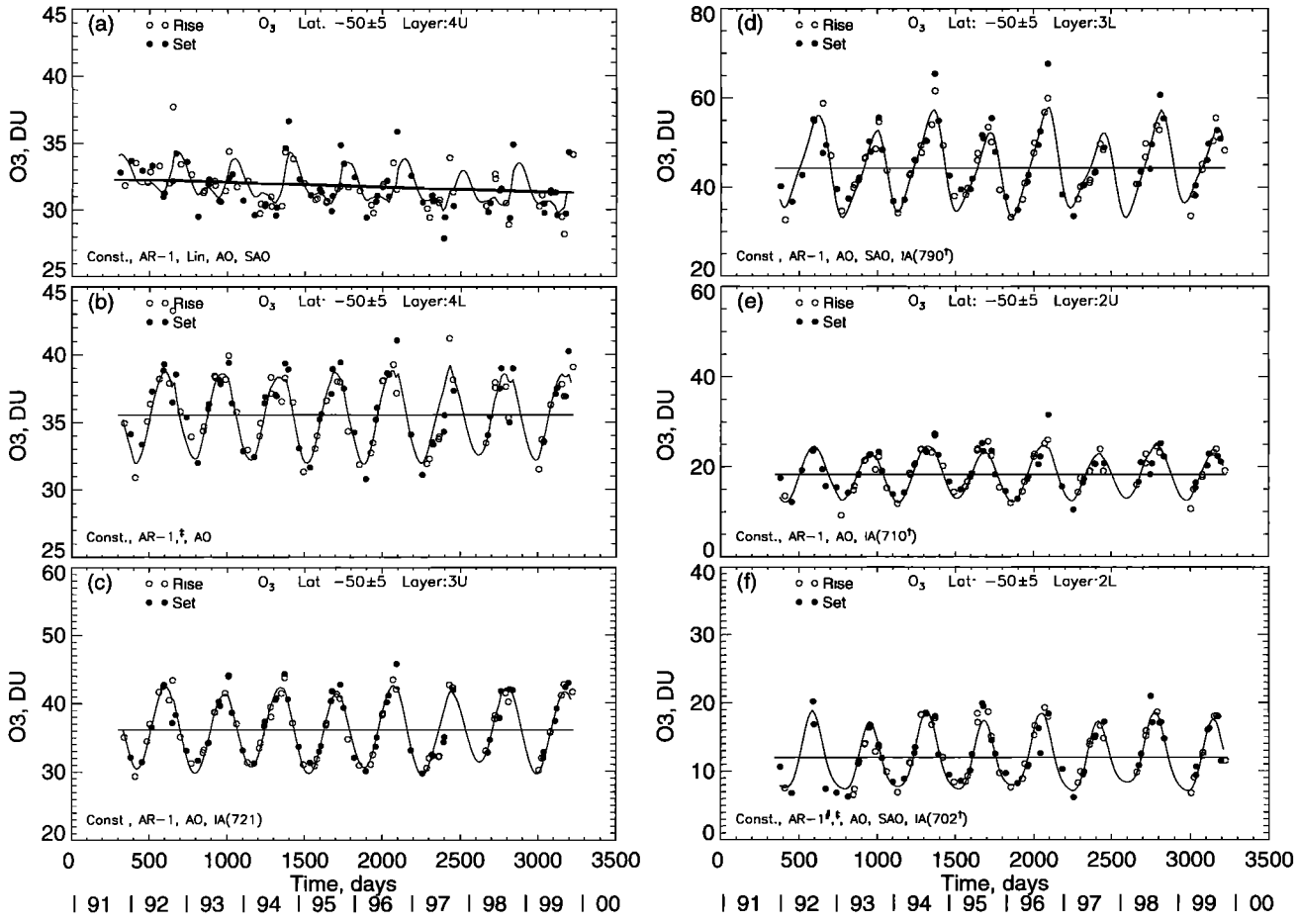

Figure 9. As in Figure 3 but for 50°S.

eruption of Mount Pinatubo in 1991, followed by a slight recovery [*Randel et al.*, 1995], and there is weak evidence of this behavior in layer 4U at 50°N in our time series of zonal average ozone. The TOMS ozone record from 1979 onward shows that most of the long-term, midlatitude ozone loss occurred in the 1980s and early 1990s, followed by an apparent increase in the middle to late 1990s [see *WMO*, 1999, Figure 4.1]. However, there was a gap from October 1994 to August 1996 between the Meteor 3 and Earth Probe TOMS observations, causing some concern about the validity of the increase in the middle 1990s.

Because HALOE ozone is increasing in layer 2 at 50°N, the effect of that change may also show up in the trends for a deeper column of HALOE ozone. We integrated the HALOE ozone over most of the stratosphere (from 253 to 7.9 hPa) at 50°N, giving an annual average ozone of 266 DU, as shown in Table 8. The integration was not extended above the 7.9-hPa level to avoid the small, direct effects of a solar cycle forcing. Nearly 40 DU of ozone occur above the 7.9-hPa level, and ~30 DU occur below the 253-hPa level. Our estimate of annual total column ozone is therefore 336 DU, which is in reasonable agreement with values from ground-based Dobson and TOMS measurements. The MLR model fit to our stratospheric column amount is shown in Figure 10, and its terms are given in Table 8. AO and AR-1 terms are indicated, and the AR term accounts for most of the low-wavenumber structure in the

Table 8. Column 253.31–7.92 hPa for 50°N ± 5° With 99 Data Points, Time Series Mean of 265.59 DU, Start Day 633.88, and Last Day 3217.38[a]

Term	Coefficient	σ	PROC	CI,[b] %	dPROC	CI, %
Constant	184.44	...	...	...	...	...
AR-1	0.29	0.10	0.66	100	0.15	85
AO	30.46	0.00	0.85	100	0.83	100
IA (645[c])	−5.53	0.19	−0.42	100	−0.34	100

[a]Lag 1, rank correlation is 0.239, and significance is 98.12; for lag 2, rank correlation is 0.055, and significance is 0.32. The length of data is 2583.50 days, and 91.27% of the data are fitted by this model. The calculated F value is 192.52, and the F distribution table F value is 3.22.

[b]Probability $1 - \alpha$ (see text).

[c]Period of the IA term is optimized.

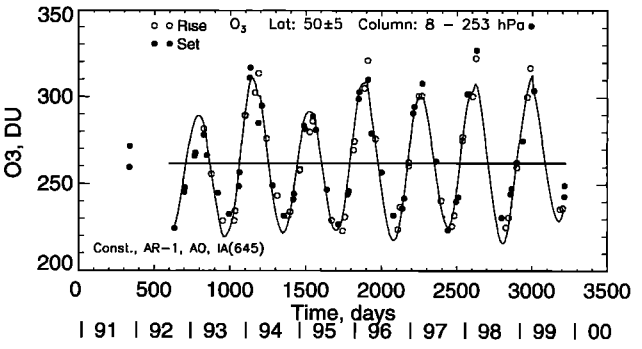

Figure 10. As in Figure 8 but for a single deep layer from 7.9 to 253 hPa at 50°N.

residuals. An IA term is present with a period of 645 days (21 months). This is the only instance where we found an IA period that short, indicating that it is more characteristic of the middle than the lower stratosphere. No significant long-term loss or increase was found, in general agreement with the results for total column ozone in the 1990s from the ground-based Dobson network at middle latitudes [see *WMO*, 1999, Figure 4-14]. Over 91% of the HALOE data is fit by this model, and the calculated F statistic is 193. Thus, either the small increase in layer 2 for HALOE is not significant in our deep column estimate or there is some compensation from the layers in the middle stratosphere. Figure 10 shows that the springtime maximum is nearly 20 DU higher in 1996 than in 1995. Such an IA variation can easily explain the apparent 1.5% upward shift in TOMS total column ozone at northern midlatitudes from the end of the Meteor 3 to the beginning of the Earth Probe record.

To summarize, time series of HALOE ozone profiles were screened of pronounced volcanic aerosol, cirrus, and tropospheric water vapor signatures and then vertically integrated into pressure layers in the lower stratosphere from 55°S to 55°N. The dominant periodic terms in this region are due to annual and interannual oscillations, which we modeled concurrently for each layer and latitude zone using MLR techniques. This method enabled us to retain the irregular spacings for the points in the time series and to account for their periodic structure more accurately. We examined the data minus model residuals for any remaining structure and included those terms that were highly significant. The periods of the interannual (or quasi-biennial) term have been determined from a Fourier analysis of the residuals in each case. This approach has made it possible to pull out any long-term ozone changes with confidence from an occultation data set.

We have focused our HALOE ozone studies on the stratosphere from 32 to 253 hPa and toward latitudes (30°N, 0, 30°S, 50°S) where ozonesonde time series are lacking or may not be so representative of zonal mean trends. We also focused on altitudes below 20.5 km, where trends in ozone are not accurate from the SAGE II version 5.96 data set [*Randel and Wu*, 1999; *Cunnold et al.*, 2000a]. Our analyses for 50°N for the early 1990s compare well with those from ozonesondes and from Dobson total column ozone. One aspect of our results that is particularly interesting is that the periodic structures and trends in the ozone time series are not seasonally symmetric at the same latitudes of the Northern and Southern Hemispheres, indicating that the effects of transport are hemispherically different [see also *Cunnold et al.*, 2000a]. For example, at 30° latitude the hemispheric differences are due to the interaction of the IA cycle with the respective AO cycles. In this regard, the HALOE results represent new estimates of the variations of zonal mean ozone within Umkehr layers 3 and 2.

First, we summarize the findings for the periodic terms for the same latitudes of each hemisphere. At 50° latitude the amplitudes of the AO terms are ~20% larger in the north than in the south. SAO and IA terms occur at both 50°N and 50°S, though not in every layer, and they are much weaker than the AO term. In contrast, the amplitudes of the AO terms at 30°N are less than half those at 30°S in layers 4L–2U, while the amplitudes of the IA terms are nearly alike. As a result, the role of the IA term is more important at 30°N. Thus there is a clear hemispheric asymmetry in the effects of transport on ozone at subtropical latitudes. Results in the tropics show a transition from transport that is dominated by the IA terms in layer 4 to seasonal transport in layer 3L. A change of phase with altitude is also indicated for the IA term at the lower latitudes.

Next, we summarize the polynomial or long-term changes in ozone at 50° latitude. We find no long-term linear loss of ozone for the decade of the 1990s at low and middle latitudes, except in layer 4U (32–45 hPa) at 50°S. The ozone decline (−0.5% yr^{-1}) at 50°S is likely related to its repeating springtime chemical loss at polar latitudes plus the effects of enhanced meridional transport following each year's final warming. There is one caution about the trend at 50°S. The HALOE measurements generally repeat at the same latitudes each year but with a lag of 4 days for each succeeding year. If the outflow from the vortex and inflow from lower latitudes occur at the same time each year, the annual precession of the sampling can alias the filaments of air from the edges of the vortex. Our inability to determine these rapid variations better represents a limitation of occultation sampling. A longer time series is needed for a better determination of this decline [*Weatherhead et al.*, 1998]. At 50°N, there is a quadratic decline of ozone in layer 4U that weakens in the second half of the 1990s. There are no significant polynomial changes in layers 4L–3L. Ozone is definitely increasing in layers 2U and 2L at 50°N, suggesting the effects of increasing diabatic descent (see Figure 1). The rate in layer 2L is +3.7% yr^{-1}. Temperatures have been decreasing in the lower stratosphere [*WMO*, 1999; *Pawson and Naujokat*, 1999], but we have not attempted a correlation between the long-term changes in HALOE ozone and lower stratospheric temperatures. It is likely that there would be uninterrupted descent in winter near the periphery of the associated, more stable polar vortex.

Finally, there are no highly significant polynomial terms in the linear models for 30° latitude, except in layer 2L at 30°N. The trend in layer 2L is consistent with that at 50°N, and both are likely affected by a change in the net circulation of the Northern Hemisphere lower stratosphere. There has been no long-term linear change in lower stratospheric tropical ozone over this 8-year period. Our lowest tropical layer 3L shows decreasing ozone in the early 1990s but increasing ozone in the late 1990s. It is concluded that much of the reported declines in lower stratospheric ozone since 1979 have occurred in the 1980s and just following the eruption of Pinatubo in the early 1990s.

Acknowledgments. We thank Jim Russell III (Principal Investigator) and the entire HALOE Project Team for producing the high-

quality level 2 ozone data set used for these studies. Geoffrey Considine advised us on the methods for significance testing that we employed in this study. He also emphasized that occultation data must be treated more generally in time series analyses. Bill Randel supplied time series of tropical wind data for testing the effects of the observed QBO wind cycle in our regression fit, and we thank him. This research has been supported with funds from a NASA NRA for UARS Science Studies managed by Joe McNeal and Mike Kurylo.

References

Baldwin, M. P., and T. J. Dunkerton, Biennial, quasi-biennial, and decadal oscillations of potential vorticity in the northern stratosphere, *J. Geophys. Res.*, *103*, 3919–3928, 1998.

Bhatt, P. P., E. E. Remsberg, L. L. Gordley, J. M. McInerney, V. G. Brackett, and J. M. Russell III, An evaluation of the quality of HALOE ozone profiles in the lower stratosphere, *J. Geophys. Res.*, *104*, 9261–9275, 1999.

Bodeker, G. E., I. S. Boyd, and W. A. Matthews, Trends and variability in vertical ozone and temperature profiles measured by ozonesondes at Lauder, New Zealand: 1986–1996, *J. Geophys. Res.*, *103*, 28,661–28,681, 1998.

Bruehl, C., S. R. Drayson, J. M. Russell III, P. J. Crutzen, J. McInerney, P. N. Purcell, H. Claude, H. Gernand, T. McGee, I. McDermid, and M. R. Gunson, HALOE ozone channel validation, *J. Geophys. Res.*, *101*, 10,217–10,240, 1996.

Considine, G., L. Deaver, E. Remsberg, and J. M. Russell III, HALOE observations of a slowdown in the rate of increase of HF in the lower mesosphere, *Geophys. Res. Lett.*, *24*, 3217–3220, 1997.

Considine, G., L. Deaver, E. Remsberg, and J. Russell III, Analysis of near-global trends and variability in HALOE HF and HCl data in the middle atmosphere, *J. Geophys. Res.*, *104*, 24,297–24,308, 1999.

Cunnold, D. M., H. J. Wang, L. W. Thomason, J. M. Zawodny, J. A. Logan, and I. A. Megretskaia, SAGE (version 5.96) ozone trends in the lower stratosphere, *J. Geophys. Res.*, *105*, 4445–4457, 2000a.

Cunnold, D. M., M. J. Newchurch, L. E. Flynn, H. J. Wang, J. M. Russell, R. McPeters, J. M. Zawodny, and L. Froidevaux, Uncertainties in upper stratospheric ozone trends from 1979 to 1996, *J. Geophys. Res.*, *105*, 4427–4444, 2000b.

Draper, N. R., and H. Smith, *Applied Regression Analysis*, John Wiley, New York, 1967.

Fusco, A. C., and M. L. Salby, Interannual variations of total ozone and their relationship to variations of planetary wave activity, *J. Clim.*, *12*, 1619–1629, 1999.

Gage, K. S., and G. C. Reid, Solar variability and the secular variation in the tropical tropopause, *Geophys. Res. Lett.*, *8*, 187–190, 1981.

Hervig, M., and M. McHugh, Cirrus detection using HALOE measurements, *Geophys. Res. Lett.*, *26*, 719–722, 1999.

Hervig, M. E., J. M. Russell III, L. L. Gordley, J. Daniels, S. R. Drayson, and J. H. Park, Aerosol effects and corrections in the Halogen Occultation Experiment, *J. Geophys. Res.*, *100*, 1067–1079, 1995.

Logan, J., An analysis of ozonesonde data for the troposphere: Recommendations for testing 3-D models and development of a gridded climatology for tropospheric ozone, *J. Geophys. Res.*, *104*, 16,115–16,149, 1999.

Luo, M., J. M. Russell III, and T. Y. W. Huang, Halogen Occultation Experiment observations of the quasi-biennial oscillation and the effects of Pinatubo aerosols in the tropical stratosphere, *J. Geophys. Res.*, *102*, 19,187–19,198, 1997.

McPeters, R. D., D. F. Heath, and P. K. Bhartia, Average ozone profiles for 1979 from the NIMBUS 7 SBUV instrument, *J. Geophys. Res.*, *89*, 5199–5214, 1984.

McPeters, R. D., S. M. Hollandsworth, L. E. Flynn, J. R. Herman, and C. J. Seftor, Long-term ozone trends derived from the 16-year combined Nimbus 7/Meteor 3 TOMS Version 7 record, *Geophys. Res. Lett.*, *23*, 3699–3702, 1996.

Mueller, R., P. J. Crutzen, J.-U. Grooss, C. Bruehl, J. M. Russell III, H. Gernandt, D. S. McKenna, and A. F. Tuck, Severe chemical ozone loss in the Arctic during the winter of 1995–1996, *Nature*, *389*, 709–712, 1997.

Nedoluha, G. E., R. M. Bevilacqua, R. M. Gomez, D. E. Siskind, B. C. Hicks, J. M. Russell III, and B. J. Connor, Increases in middle atmosphere water vapor as observed by the Halogen Occultation Experiment and the ground-based water vapor millimeter-wave spectrometer from 1991 to 1997, *J. Geophys. Res.*, *103*, 3531–3544, 1998.

Pan, L., S. Solomon, W. Randel, J.-F. Lamarque, P. Hess, J. Gille, E.-W. Chiou, and M. P. McCormick, Hemispheric asymmetries and seasonal variations of the lowermost stratospheric water vapor and ozone derived from SAGE II data, *J. Geophys. Res.*, *102*, 28,177–28,184, 1997.

Pawson, S., and B. Naujokat, The cold winters of the middle 1990s in the northern lower stratosphere, *J. Geophys. Res.*, *104*, 14,209–14,222, 1999.

Perliski, L. M., S. Solomon, and J. London, On the interpretation of seasonal variations of stratospheric ozone, *Planet. Space Sci.*, *37*, 1527–1538, 1989.

Press, W. H., B. P. Flannery, S. A. Teukolsky, and W. T. Vetterling, *Numerical Recipes*, Cambridge Univ. Press, New York, 1988.

Randel, W. J., and F. Wu, A stratospheric ozone trends data set for global modeling studies, *Geophys. Res. Lett.*, *26*, 3089–3092, 1999.

Randel, W. J., F. Wu, J. M. Russell III, J. W. Waters, and L. Froidevaux, Ozone and temperature changes in the stratosphere following the eruption of Mount Pinatubo, *J. Geophys. Res.*, *100*, 16,753–16,764, 1995.

Randel, W. J., F. Wu, J. M. Russell III, A. Roche, and J. W. Waters, Seasonal cycles and QBO variations in stratospheric CH4 and H2O observed in UARS HALOE data, *J. Atmos. Sci.*, *55*, 163–185, 1998.

Randel, W. J., R. S. Stolarski, D. M. Cunnold, J. A. Logan, M. J. Newchurch, and J. Zawodny, Trends in the vertical distribution of ozone, *Science*, *285*, 1689–1692, 1999.

Rosenlof, K. H., Seasonal cycle of the residual mean meridional circulation in the stratosphere, *J. Geophys. Res.*, *100*, 5173–5191, 1995.

Russell, J. M., L. L. Gordley, J. H. Park, S. R. Drayson, W. D. Hesketh, R. J. Cicerone, A. F. Tuck, J. E. Frederick, J. E. Harries, and P. J. Crutzen, The Halogen Occultation Experiment, *J. Geophys. Res.*, *98*, 10,777–10,797, 1993.

Steele, H. M., and R. T. Turco, Separation of aerosol and gas components in the Halogen Occultation Experiment and the Stratospheric Aerosol and Gas Experiment (SAGE II) extinction measurements: Implications for SAGE II ozone concentrations and trends, *J. Geophys. Res.*, *102*, 19,665–19,682, 1997.

Stratospheric Processes and Their Role in Climate (SPARC), Assessment of trends in the vertical distribution of ozone, edited by N. Harris, R. Hudson, and C. Phillips, *SPARC Rep. 1*, 289 pp., Verrières-le-Buisson, France, 1998.

Tiao, G. C., G. C. Reinsel, D. Xu, J. H. Pedrick, X. Zhu, A. J. Miller, J. J. DeLuisi, C. L. Mateer, and D. J. Wuebbles, Effects of autocorrelation and temporal sampling schemes on estimates of trend and spatial correlation, *J. Geophys. Res.*, *95*, 20,507–20,517, 1990.

Tung, K. K., and H. Yang, Global QBO in circulation and ozone, part I, Reexamination of observation evidence, *J. Atmos. Sci.*, *51*, 2699–2707, 1994.

Wang, P.-H., D. M. Cunnold, J. M. Zawodny, R. B. Pierce, J. R. Olson, G. S. Kent, and K. M. Skeens, Seasonal ozone variations in the isentropic layer between 330 and 380K as observed by SAGE II: Implications of extratropical cross-tropopause transport, *J. Geophys. Res.*, *103*, 28,647–28,659, 1998.

Weatherhead, E. C., et al., Factors affecting the detection of trends: Statistical considerations and applications to environmental data, *J. Geophys. Res.*, *103*, 17,149–17,161, 1998.

World Meteorological Organization (WMO), Scientific assessment of ozone depletion: 1998, *Global Ozone Res. Monit. Proj. Rep. 44*, Geneva, 1999.

P. P. Bhatt, Science Applications International Corporation, One Enterprise Plaza, Hampton, VA 23666. (p.p.bhatt@larc.nasa.gov)

L. E. Deaver and E. R. Remsberg, Atmospheric Sciences Research, NASA Langley Research Center, MS 401B, 21 Langley Blvd., Hampton, VA 23681. (l.e.deaver@larc.nasa.gov; e.e.remsberg@larc.nasa.gov)

(Received March 7, 2000; revised July 10, 2000;
accepted August 29, 2000.)